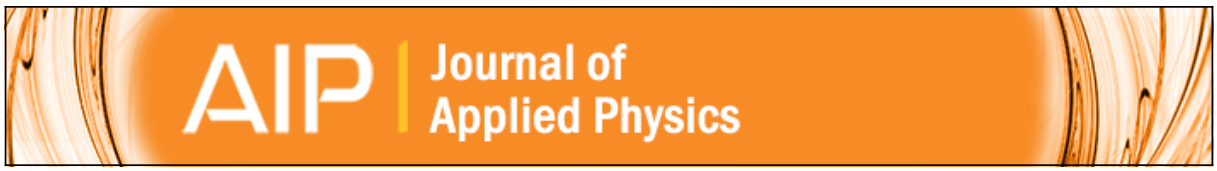

Real-time monitoring of nucleation-growth cycle of carbon nanoparticles in acetylene plasmas

Morten Hundt, Patrick Sadler, Igor Levchenko, Matthias Wolter, Holger Kersten, and Kostya (Ken) Ostrikov

Citation: Journal of Applied Physics **109**, 123305 (2011); doi: 10.1063/1.3599893

View online: http://dx.doi.org/10.1063/1.3599893

View Table of Contents: http://scitation.aip.org/content/aip/journal/jap/109/12?ver=pdfcov

Published by the AIP Publishing

Real-time monitoring of nucleation-growth cycle of carbon nanoparticles in acetylene plasmas

Morten Hundt,[1] Patrick Sadler,[1] Igor Levchenko,[2,3] Matthias Wolter,[1,2] Holger Kersten,[1] and Kostya (Ken) Ostrikov[2,3,a)]
[1]*Institute of Experimental and Applied Physics, University Kiel, D-24098 Kiel, Germany*
[2]*Plasma Nanoscience Centre Australia (PNCA), CSIRO Materials Science and Engineering, Lindfield, New South Wales 2070, Australia*
[3]*Plasma Nanoscience, School of Physics, The University of Sydney, Sydney, New South Wales 2006, Australia*

(Received 29 March 2011; accepted 12 May 2011; published online 28 June 2011)

Quantum cascade laser absorption spectroscopy was used to measure the absolute concentration of acetylene *in situ* during the nanoparticle growth in $Ar + C_2H_2$ RF plasmas. It is demonstrated that the nanoparticle growth exhibits a periodical behavior, with the growth cycle period strongly dependent on the initial acetylene concentration in the chamber. Being 300 s at 7.5% of acetylene in the gas mixture, the growth cycle period decreases with the acetylene concentration increasing; the growth eventually disappears when the acetylene concentration exceeds 32%. During the nanoparticle growth, the acetylene concentration is small and does not exceed 4.2% at radio frequency (RF) power of 4 W, and 0.5% at RF power of 20 W. An injection of a single acetylene pulse into the discharge also results in the nanoparticle nucleation and growth. The absorption spectroscopy technique was found to be very effective for the time-resolved measurement of the hydrocarbon content in nanoparticle-generating plasmas. © *2011 American Institute of Physics*. [doi:10.1063/1.3599893]

I. INTRODUCTION

Low-temperature, low-pressure plasmas have been successfully used in nanoscale synthesis and processing over the last few years.[1–5] The plasma-grown nanostructures demonstrate numerous unique properties (high degree of crystallinity, density, etc.) that cannot be achieved using neutral gas-based techniques. These properties provide excellent opportunities for the use of these nanostructures in various nanoscale devices, such as tips of the atomic force microscopy, nano-electronic and optoelectronic devices, photovoltaic solar cells and others.[6,7] For the best use of these plasma-grown nanostructures, their properties (especially size, shape, and crystallinity) should be precisely controlled during the fabrication.[8,9] This in turn means that the stages of nanostructure nucleation and growth should be precisely monitored directly in the reactor chamber. This is an extremely hard task since the technological process is usually conducted in low-pressure plasma discharges that produce intense light and heat fluxes.

Among other plasma-grown nanostructures, the nanodust (nanoparticles grown directly in the plasma bulk) represent a special interest due to their unique properties and applications in nanoscale assembly by precise deposition onto the specific locations using specially shaped electric fields.[10–12] The nucleation and growth of the nanodust grains in plasmas were observed and studied previously.[13–15] Nanoparticle growth is usually a very fast and a complex multistage process which is very difficult to monitor. Most of the present-day diagnostic techniques still lack reliability and require further development. For an improved insight in the plasma-polymerization processes, especially to determine the key precursors in the carbonaceous dusty plasmas, mass spectrometry has been successfully used by several research groups.[16–18] Nevertheless, a quantitative mass spectrometry is a very complex technique.

One of the important tasks is real-time monitoring of the gas and plasma parameters (pressure, density, chemical composition) directly in the discharge where the nanodust nucleates and grows. Besides, these measurements are extremely complex for the molecular plasmas which are increasingly used in the nanomaterial synthesis technology due to their extraordinary reactivity and other favorable characteristics.[19]

There have been several attempts to describe the plasma chemistry in nanoparticle-generating hydrocarbon plasmas.[20–22] A mass spectrometry was used to study the role of positive ions on the chemistry of RF discharges in acetylene.[23] For pure acetylene discharge they found positive ions up to $C_6H_2^+$ with the most common being $C_4H_2^+$ and $C_4H_3^+$. Platzner and Marcus studied the neutral gas distribution in a microwave discharge and discussed the reactions that initiate dust growth.[24] Doyle considered the most important reactions in a plasma and compared the results with the experimentally measured partial pressures of H_2 and C_nH_2, where $n = 2, 4, 6$ (Ref. 25). There were also attempts to describe the growth of initial nuclei.[26,27] Despite these numerous efforts, the nanodust nucleation and growth kinetics is still not clear and requires further investigations.

The commonly used probe technique is cheap and simple, but it exhibits low accuracy due to the probe effect on the plasma and strong heating of the probe electrode in the discharge. In the processes utilizing hydrocarbon and silicon-organic plasmas, the infrared absorption spectroscopy

a)Author to whom correspondence should be addressed. Electronic mail: Kostya.Ostrikov@csiro.au.

techniques could be successfully used since these molecules or their constituents are active in the infrared spectral region.

The Fourier transform infrared spectroscopy (FTIR) is a common and effective method for *in situ* analysis of C_xH_y plasmas, but it still lacks sensitivity in the required nanoparticle size range[28] unless a multi-pass arrangement was used to enhance the FTIR signal sensitivity.[29] Another possible technique is the tunable diode laser absorption spectroscopy (TDLAS) which is a convenient method for measuring the concentrations of free radicals, transient molecules and stable products in the spectral region between 3 and 20 μm. The TDLAS can also be successfully used to measure neutral gas temperature[30] and to investigate dissociation processes in low-temperature molecular plasmas.[31–33]

In this work we have used a compact transportable measurement equipment named "Quantum Cascade Laser Measurement and Control System" (Q-MACS) developed by Neoplas Control GmbH. This system provides an effective and reliable real-time plasma diagnostics and process control. The Q-MACS is based on recent developments in pulsed quantum cascade lasers (QCLs), and offers new possibilities for infrared absorption spectroscopy.[34–36] The QCLs are able to emit mid-infrared radiation under near-room-temperature operation conditions. More details on the commercially available Q-MACS systems can be found elsewhere.[37] Here, we have used the Q-MACS systems to measure the *absolute C_2H_2 concentration* directly in the discharge, in real time, to quantify the kinetics of the nanoparticle nucleation, growth, and precipitation in low-temperature RF plasmas. It is shown that the period of the nanoparticle formation depends on the plasma discharge power and the precursor gas concentration. Experiments on the momentary acetylene injection in the discharge also demonstrate the possibility to control the nanodust formation.

II. EXPERIMENTAL SETUP AND PROCEDURES

The experiments were performed in a specially designed setup consisting of a vacuum chamber, vacuum pump, gas supply, and two characterization facilities: laser diode-detector system for the detection of nanoparticles nucleated and growing in the plasma, and Q-MACS capable of measuring the plasma parameters (see Fig. 1). The experiments have been performed in an asymmetric radio-frequency (RF) discharge at 13.56 MHz. Argon and acetylene were used as a background gas and a reactive precursor, respectively. All experiments were conducted at a total pressure of 5.5 Pa. The acetylene flow was varied between 0 and 1.75 sccm in different series of measurements. To keep the total pressure constant, the argon flow was adjusted manually with a needle valve. The turbo-molecular pump has a throughput of 1 mbar $\times$ s^{-1} at the operating pressure, which means the gas residence time in order of 1 s for the incoming gas flow rates and the vessel volume. The RF power was varied in the range of 4 to 20 W. For these operating conditions, the positive ion density and particle concentrations of 10^9 cm^{-3} and 10^7 cm^{-3}, respectively, were estimated. These numbers are in a good agreement with the measurements made in the similar experimental setup, at the similar discharge conditions.[38]

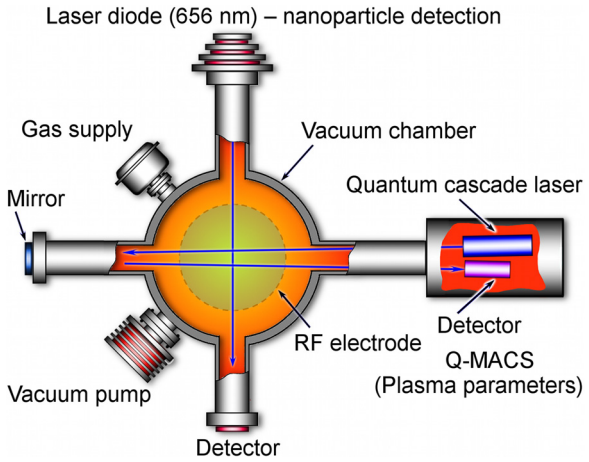

FIG. 1. (Color online) Schematic of the experimental set-up. The laser diode-based system is used to illuminate the dust and measure the dust density in the plasma. The Q-MACS system provides information about time-dependent C_2H_2 concentration in the plasma.

The absolute C_2H_2 concentration inside the vessel was measured *in situ* by Q-MACS. Through a current ramp, the pulsed QCL (pulse width 12 ns) can be tuned with a rate of 0.25 cm^{-1} within a spectral range of 1340 cm^{-1} to 1344 cm^{-1}, where several spectral lines of the infrared (IR)-active acetylene molecule are available. The absolute acetylene molecule concentration in the chamber was measured using the spectral line 1342.35 cm^{-1}. This absorption line was identified as the rotational-vibrational transition from the ground level to the first excited state of the two bending modes $\nu_4 + \nu_5$ (J = 5 $\rightarrow$ 6) (Ref. 39). To calculate the absolute C_2H_2 concentration in the vacuum chamber, the passing absorption signal was analytically fitted and internally compared with spectral data from the high-resolution transmission molecular absorption (HITRAN) database.[40]

The nanoparticles in the plasma were studied using transmitted light of a 658 nm laser detected by a photodiode connected to an integrated amplifier. The intensity of the beam passing through the plasma decreases during the particle formation due to scattering on their surfaces, thus indicating the nanodust formation.

III. EXPERIMENTAL RESULTS

In Fig. 2(a), we show a photograph of the plasma region, where the clouds of nucleated dust particles illuminated by a laser beam are clearly visible. Moreover, a particle-free region, commonly known as a void, can be observed between the two clouds. We have observed that the volume of the void increased during the dust growth cycle, and the boundary moved toward the electrode edge. The plasma-grown dust particles precipitate to the lower electrode after growing above the upper mass limit resulting in the associated disturbance of levitation conditions, and can be collected on the electrode surface. In Fig. 2(b), we show a SEM image of typical carbon nanoparticles collected on the particle collector.

The simultaneously measured time dependencies of the total pressure in the vacuum chamber, RF electrode self-bias voltage, transmitted laser light intensity (which directly

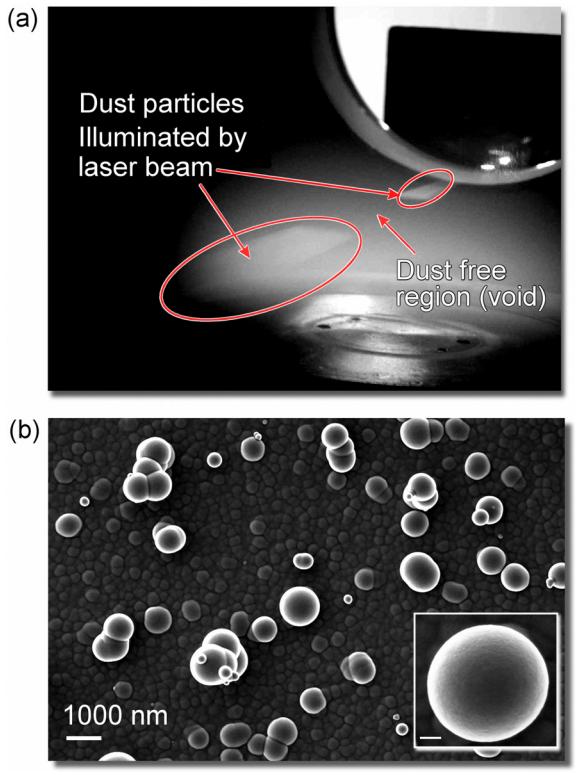

FIG. 2. (Color online) (a) Photo of a dust cloud in the plasma illuminated by the laser diode. The void (a region free of any particles) is clearly visible in the center, above the powered electrode; (b) SEM image of the typical carbon nanoparticles collected on the particle collector. The scale bar in the inset is 200 nm.

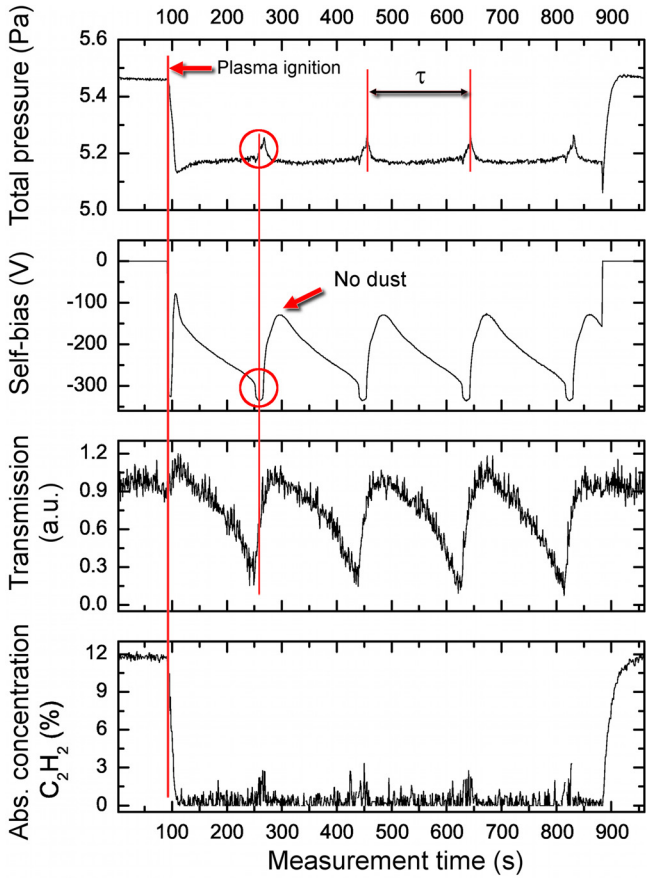

FIG. 3. (Color online) Comparison of the measurements of the total pressure, the self-bias voltage at the powered RF electrode, the transmitted laser light, which corresponds directly with the density of the spontaneously generated dust particles, and the absolute C_2H_2 concentration in the experiment. The observation of all of the different parameters show the same effect in the periodic behavior in the discharge. The growth cycle period τ for all observed parameters is equal.

corresponds to the density of dust particles in the plasma), and the absolute concentration of acetylene during the particle formation process are shown in Fig. 3.

At the beginning of this experiment, the total pressure was 5.5 Pa and the acetylene concentration was 12%. When the plasma (RF discharge) was switched on, the self-bias voltage abruptly dropped down to − 330 V. The total gas pressure and the absolute C_2H_2 concentration have also demonstrated a similar behavior, dropping immediately from 5.5 to 5.1 Pa, and from 12% to near zero, respectively. After a few seconds into the process, the transmitted laser light intensity also started to decrease slowly, thus clearly indicating the formation of dust particles in the plasma. During the next 170 s, the self-bias voltage and the laser light transmission decrease continuously, with the pressure slightly increasing (probably due to the changes in the molecule number density due to chemical reactions). The concentration of acetylene was nearly constant at a rather low (0–0.5%) level.

When the laser light transmission reached the minimum, a sudden jump in all measured signals was observed. Indeed, the self-bias potential has shown an abrupt drop by approximately 50 V followed by the rapid recovery to −150 V; the total pressure in the chamber and acetylene concentration responded with small, but clearly noticed peaks. After that, the transmitted light intensity signal increased sharply and eventually reached the initial level, thus indicating that the line of laser beam sight is dust-free, due to the dust precipitation onto the electrode surface. A further experiment has demonstrated that the cycle of dust formation, self-bias build-up, and transmitted light intensity oscillations continue repeatedly with a stable period.

A series of measurements of the transmitted light intensity oscillations with different initial acetylene concentrations (from 17.5% to 32%) were performed at a constant RF power of 10 W. To setup the initial acetylene concentration, the gas flow ratio of Ar and C_2H_2 before the plasma ignition was regulated. The graph of the obtained dependencies is shown in Fig. 4 This graph shows the oscillating behavior of the transmitted light (and hence, the dust density) at a concentration of 29%. This behavior was seen for acetylene concentrations between 17 and 30%. With the acetylene concentration increasing, the growth cycle duration and the signal amplitude decrease. The oscillations become more frequent and smooth, and finally, the periodic behavior terminates at the acetylene concentration of about 32%. Interestingly, even at the high acetylene concentration of about 32% (not supporting the periodic growth behavior) the system shows several high-amplitude oscillations, which later decay after reaching some transmission level. It is also notable that this equilibrium signal level is significantly lower than the initial signal. Thus, this indicates that at the

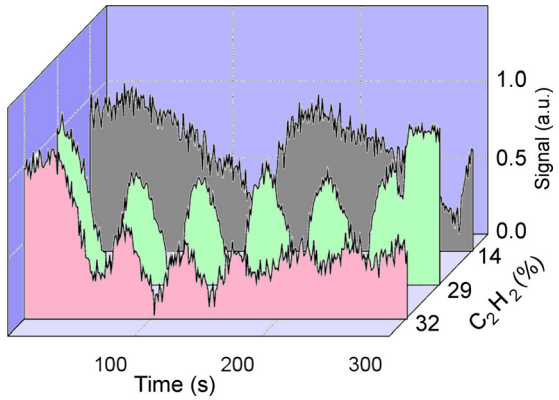

FIG. 4. (Color online) Laser light transmission signal (photodiode). When the dust cloud arises, the signal decreases. The growth cycle period decreases with the initial acetylene concentration until the periodic behavior extinguishes at the concentration of about 32%.

high acetylene concentration the particles grow continuously in the whole plasma bulk, i.e., including the void area formed at a lower acetylene concentration.

As it was mentioned above and illustrated in Fig. 3, the period of the growth cycles is constant under preset plasma conditions. To better investigate this phenomenon, we have performed a series of the experiments to determine the correlation of the nanoparticle growth cycle with the RF power and initial acetylene concentration at a constant total pressure. For this, we have measured the dependence of the growth cycle duration τ on the RF power in a plasma with an initial acetylene concentration of 17.5% and a total pressure of 5.5 Pa, with the RF power varied between 4 and 20 W.

The measured dependencies are shown in Fig. 5. With the RF power increasing, the growth period also increases and finally saturates at the power of 16 W and higher. It is clear that the increase of the discharge power results in higher dissociation rates of C_2H_2, and finally in higher concentrations of radicals such as C_2H. On the other hand, an increase of the

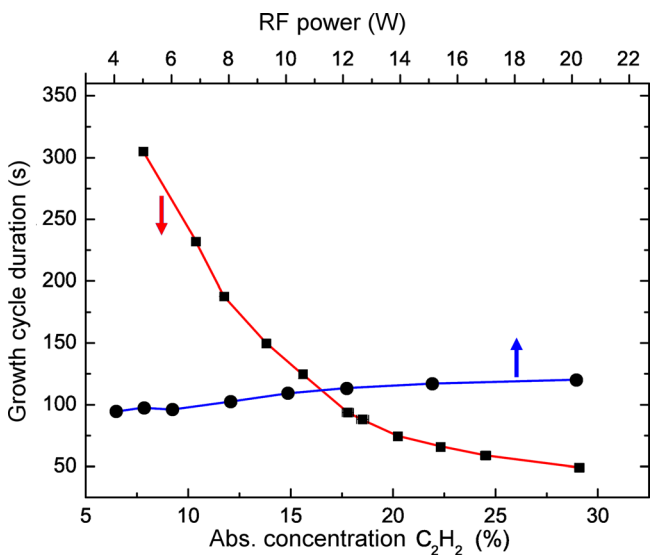

FIG. 5. (Color online) Dependencies of the growth cycle period on RF power and initial acetylene concentration. The growth cycle period weakly depends on the power and strongly depends on the initial acetylene concentration.

discharge power strongly changes the plasma parameters, and in particular, increases the electron temperature and electron density. As a result, the negative potential of the plasma-nucleated particles will also increase and finally, the flux of the reactive negative ions (such as C_2H^-, C_4H^-, etc.) to the growing particles will be reduced, eventually resulting in the decrease of the particles growth rates. Thus, the growth of particles in the plasma is a complex process that depends on the production rate of reactive molecules/radicals in the plasma, as well as the plasma parameters which govern the molecules/radicals flux to the particles.

One can assume that the dissociation rate change is low in the above power range, thus the dependence of the cycle duration on the power is weak. With the initial acetylene concentration increasing, the cycle duration decreases strongly, as a result of the increase in the molecular flux to the dust particles. However, when the initial acetylene concentration approaches 30%, the dust growth period saturates at about 50 s.

The time-resolved measurements of the variation of acetylene concentration during the particle growth cycle have shown that when the initial concentration is below 20%, a rather small amount (about 0.5% for the initial concentration of 12%, as shown in Fig. 3) of acetylene is present in the plasma, which is still sufficient to initiate the nucleation and sustain the growth in the cyclic mode. In this case, quite noticeable peaks (up to 2–3%) of the acetylene density at the time moments corresponding to the low particle density herald the onset of the nucleation of new particles and therefore the commencement of the new growth cycle. Similar measurements conducted in the process with the initial acetylene concentration above 20% have shown that a significant amount of acetylene was present in the plasma during the whole growth cycle. In this case, the particle growth rate was higher and hence the growth cycle duration was smaller. When the initial concentration of acetylene was above 32%, the oscillating behavior disappeared.

The equilibrium acetylene concentration in the plasma also depends on the RF power applied to the discharge. In Fig. 6 we show the acetylene concentration—RF power dependence measured for the initial C_2H_2 concentration of 17.5% and the total gas pressure of 5.5 Pa. At low powers of 4–10 W, the equilibrium C_2H_2 concentration is relatively high (4 to 1%), whereas it falls down to 0.5% at 20 W. This result supports our opinion that the higher discharge power leads to the higher dissociation rate of acetylene, and hence, higher concentration of various radicals and ions in the plasma. This will, in turn, strongly change the plasma parameters and particle growth conditions and eventually, result in a slight increase in the growth cycle duration due to changed conditions of the radicals and ions supply to the growing particles, as we discussed in details above.

To extend the above described measurements conducted at a constant acetylene flow, an additional experiment has been performed with one single pulse of acetylene injected into the argon discharge. In Fig. 7, the time dependencies of the total pressure, self-bias voltage of the RF electrode, and absolute concentration of acetylene are shown. During this experiment, the RF power and argon gas pressure were 10 W and 5.6 Pa, respectively.

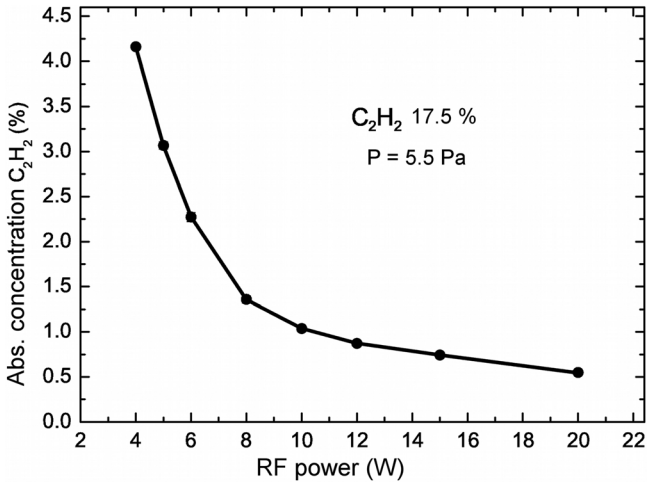

FIG. 6. Dependence of the absolute acetylene concentration in the discharge on the RF power. The total pressure (5.5 Pa) and the initial acetylene concentration (17.5%) were constant during the experiment. The C_2H_2 concentration decreases with the RF power increasing.

In this experiment, the acetylene flow during the pulse was 8 sccm, which corresponds to the absolute concentration of 17% in a steady-state operation without a plasma. Shortly after the injection of the C_2H_2 pulse, the total pressure in the chamber rises to 6.8 Pa, and the self-bias voltage starts decreasing thus heralding the commencement of the dust formation process. In 10 s after the acetylene injection, no C_2H_2 is detected in the discharge. After that, the self-bias voltage decreases very slowly down to −180 V, indicating that the dust particles are levitating in the sheath. Finally, after nearly 700 s, the self-bias voltage suddenly drops down to the initial value due to the precipitation of the remaining dust from the plasma. After that, the argon discharge appears to be free of dust. An experiment in an Ar/CH_4 discharge with a single C_2H_2 pulse has demonstrated a similar behavior: the scattered light intensity was increasing transiently and then dropped down afterwards.[29]

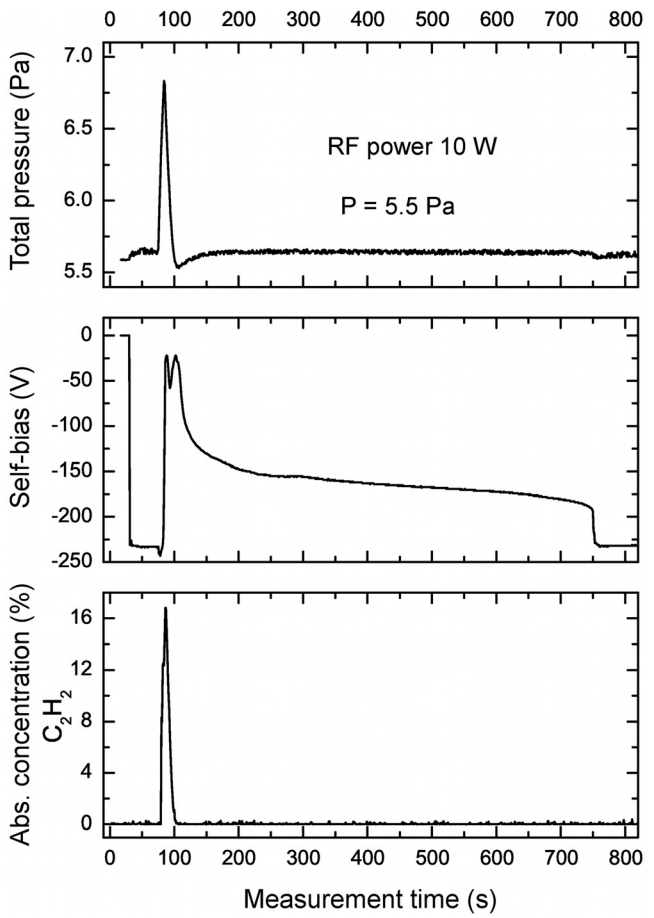

FIG. 7. Time dependencies of the RF electrode self-bias voltage, acetylene concentration, and total pressure in the chamber for an argon plasma with injected acetylene pulse. The changes in the absolute concentration of C_2H_2 and total pressure are clearly visible. The self-bias behavior proves the nucleation and growth on nanodust in a single growth cycle caused by the acetylene pulse injection. The particles are lost after 750 s, and the self-bias voltage returns to the initial value.

IV. DISCUSSION

Let us now discuss some interesting physical phenomena found in the experiments. The effect of the nanodust formation on the plasma characteristics was reported.[10,41] Our experiments with the Q-MACS have revealed an important feature of the temporal self-bias behavior in the nanodust growth process. Indeed, as shown in Fig. 3, the minimum of the light transmission – time curve (which corresponds to the maximum nanodust density in the plasma) corresponds to the strongly pronounced local down-shot of the self-bias – time curve, with the down-shot width exactly correlating with the duration of the transmission signal recovery to the initial (dust-free) level. It is known that the self-bias potential on the RF electrode is due to the asymmetry of the discharge, which results in biasing the electrode due to the electron flux from the plasma. The presence of a negative peak on the self-bias curve can be explained by the additional charge transfer between the dust cloud and the electrode;[42] hence, this is an evidence that the particles in the RF plasma are negatively charged. However, our estimates of the dust density show that the dust particle charge is not sufficient to completely explain the changes in RF signals. We assume that a drastic change in the discharge heating mode, i.e., transition from the ohmic to the stochastic heating, occurs in this case and eventually leads to the change in the power coupling;[43,44] nevertheless, further investigations are required to clarify this issue.

When the outward ion drag force is applied to the particles and the inward electric force become unbalanced, the particles then start to precipitate and the void is spread out over the whole electrode; a new growth cycle can then start. The dust formation starts spontaneously in the dust-free region over the powered RF electrode.[45–47] Hence, we determine three different regimes of dust formation depending on the precursor gas concentration in this plasma type: periodic, periodic-continuous, and continuous particle growth.

According to the present-day concept, the growth of particles in low-temperature plasma proceeds as follows.[46,48] After the nucleation phase, the proto-particles of a few nanometer size coagulate due to charge fluctuations[49] and can agglomerate to the size of several tens of nanometers similarly to the coagulation of neutral aerosols.[27] Advanced models provide self-consistent descriptions considering plasma effects like polarization of a particle in the vicinity of another particle

which causes an ion flow asymmetry, leading to an effective attraction between negatively charged particles.[50,51] This may lead to the gas-phase formation of the agglomerates with the sizes comparable with the sizes of particles collected in our experiments. The density of such agglomerates is quite low and is typically in the several thousand per cubic centimeter range.[50,51]Furthermore, since larger dust particles have larger collision cross-sections, they act as a sink for neutral radicals and positive ions, thus they can grow up to several hundred nanometers.[15] Because of the size-dependent force balance, the size distribution of the dust particles tends to be quite monodisperse as proven by SEM measurements and is also consistent with our results.[41]

The decrease in the acetylene concentration in the plasma can be explained by considering the details of the electron-impact ionization and dissociation. The spontaneous dust formation in the plasma bulk strongly influences the plasma parameters, especially the electron density, electron temperature, plasma impedance and chemical composition. The dusty plasma region outside the void is characterized by a low electron density and a high electron temperature.[52] The increase of the electron temperature can be explained by the loss of ions and electrons due to the recombination on the nanoparticle surfaces, which must be compensated by the increasing ionization rate in order to maintain the discharge.[53,54] Thus, the decrease of acetylene concentration is due to the strong electron impact dissociation and ionization. As a result, many species (cations, anions, neutral radicals) are produced by several reactions, for example:[55]

$$C_2H_2 + e^- \rightarrow C_2H_2^+ + 2e^- \ (Ionization) \quad (1)$$

$$C_2H_2^+ + C_2H_2 \rightarrow C_4H_2^+ + H_2 \quad (2)$$

$$C_2H_2 + e^- \rightarrow C_2H^- + H \ (Attachment) \quad (3)$$

$$C_2H^- + C_2H_2 \rightarrow C_4H^- + H_2 \quad (4)$$

$$C_2H_2 + e^- \rightarrow C_2H + H + e^- \ (Dissociation) \quad (5)$$

$$C_2H + C_2H_2 \rightarrow C_4H_2 + H \quad (6)$$

According to de Bleecker *et al.*, the C_2H^- anion produced in Eq. (3) plays an important role in triggering the formation of carbonaceous nanoparticles.[56]

IV. CONCLUSIONS

It was demonstrated that quantum cascade laser absorption spectroscopy (QCLAS) is a very useful tool to measure the absolute precursor gas concentration in nanoparticle-generating plasmas. The correlation between the particle growth period and the absolute acetylene concentration inside the plasma was measured for different RF powers and initial acetylene concentrations. It has also been shown that for absolute concentration of acetylene up to 32%, the particle growth follows a periodic behavior with decreasing the growth cycle durations. For higher absolute acetylene concentrations a continuous nanoparticle growth without periodic behavior was observed. These results, supported by the measurements of the self-bias voltage and the changes in dust density, provide insights on the self-induced phenomenon of nanoparticle growth and the periodic behavior of this process under constant plasma parameters. This is important for various applications based on the plasma-grown nanoparticles.

ACKNOWLEDGMENTS

The authors would like to thank the Leibniz-Institut für Plasmaforschung und Technologie e.V. (INP), Neoplas Control GmbH, and H. Zimmermann and V. Rohwer for the technical support. This work was supported by the German Research Foundation (DFG) within the framework of Project No. SFB-TR24 B13, the Australian Research Council, and CSIRO OCE Science Leadership Program.

[1]D. Mariotti, V. Švrček, and D.-G. Kim, Appl. Phys. Lett. **91**, 183111 (2007).
[2]K. Ostrikov, Rev. Mod. Phys. **77**, 489 (2005); J. Phys. D: Appl. Phys. **44**, 174003 (2011).
[3]A. Anders, Appl. Phys. Lett. **80**, 1100 (2002).
[4]Yu. A. Akimov, W. S. Koh, and K. Ostrikov, Opt. Express **17**, 10195 (2009); Yu. A. Akimov, K. Ostrikov, and E. P. Li, Plasmonics **4**, 107 (2009).
[5]I. Levchenko, K. Ostrikov, K. Diwan, K. Winkler, and D. Mariotti, Appl. Phys. Lett. **93**, 183102 (2008); I. Levchenko, K. Ostrikov, and A. B. Murphy, J. Phys. D: Appl. Phys. **41**, 092001 (2008).
[6]M. Keidar and I. I. Beilis, J. Appl. Phys. **106**, 103304 (2009).
[7]U. Cvelbar and M. Mozetic, J. Phys. D: Appl. Phys. **40**, 2300 (2007).
[8]I. Levchenko, K. Ostrikov, and S. Xu, J. Phys. D: Appl. Phys. **42**, 125207 (2009).
[9]M. Keidar, I. Levchenko, T. Arbel, M. Alexander, A. M. Waas, and K. Ostrikov, Appl. Phys. Lett. **92**, 043129 (2008).
[10]M. Wolter, M. Haass, T. Ockenga, J. Blazek, and H. Kersten, Plasma Processes Polym. **6**, S620 (2009).
[11]M. Wolter, I. Levchenko, H. Kersten, and K. Ostrikov, Appl. Phys. Lett. **96**, 133105 (2010).
[12]A. Anders and G. Yushkov, J. Appl. Phys. **91**, 4824 (2002).
[13]G. S. Selwyn, J. Singh, and R. S. Bennett, J. Vac. Sci. Technol. A **7**, 2758 (1989).
[14]S.-H. Hong and J. Winter, J. Appl. Phys. **100**, 064303 (2006).
[15]Ch. Hollenstein, Plasma Phys. Controlled Fusion **42**, R93 (2000).
[16]A. Consoli, J. Benedikt, and A. von Keudell, Plasma Sources Sci. Technol. **18**, 034004 (2009).
[17]A. Baby, C. M. O. Mahony and P. D. Maguire, Plasma Sources Sci. Technol. **20**, 015003 (2011).
[18]J. Benedikt, J. Phys. D: Appl. Phys. **43**, 043001 (2010).
[19]K. Vasilev, A. Michelmore, P. Martinek, J. Chan, V. Sah, H. J. Griesser, and R. T. D. Short, Plasma Processes Polym. **7**, 824 (2010).
[20]S. Stoykov, C. Eggs, and U. Kortshagen, J. Phys. D.: Appl. Phys. **34**, 2160 (2001).
[21]H. Kobayashi, A. Bel, and M. Shen, Macromolecules **7**, 277 (1974).
[22]J. M. Tibbitt, R. Jensen, A. T. Bell, and M. Shen, Macromolecules **10**, 647 (1977).
[23]M. Vasile and G. Smolinsky, Int. J. Mass Spectrom. Ion Phys. **24**, 11 (1977).
[24]I. Platzner and P. Marcus, Int. J. Mass Spectrom. Ion Phys. **41**, 241 (1982).
[25]J. Doyle, J. Appl. Phys. **82**, 4763 (1997).
[26]P. Haaland, A. Garscadden, and B. Ganguly, Appl. Phys Lett. **69**, 904 (1996).
[27]U. Kortshagen and U. Bhandarkar, Phys. Rev. E **60**, 887 (1999).
[28]C. Deschenaux, A. Affolter, D. Magni, C. Hollenstein, and P. Fayet, J. Phys. D: Appl. Phys. **32**, 1876 (1999).
[29]J. Winter, J. Berndt, S.-H. Hong, E. Kovačević, I. Stefanović and O. Stepanović, Plasma Sources Sci. Technol. **18**, 034010 (2009).
[30]M. Haverlag, E. Stoffels, W. Stoffels, G. Kroesen, and F. de Hoog, J. Vac. Sci. Technol. A **14**, 380 (1996).
[31]S. Naito, N. Ito, T. Hattori, and T. Goto, Jpn. J. Appl. Phys. **34**, 302 (1995).
[32]M. Haverlag, E. Stoffels, W. Stoffels, G. Kroesen, and F. de Hoog, J. Vac. Sci. Technol. A **12**, 3102 (1994).
[33]J. Roepcke, L. Mechold, M. Kning, W. Fan, and P. Davies, Plasma Chem. Plasma Process. **19**, 395 (1999).

[34]J. Faist, F. Capasso, D. Sivco, C. Sirtori, A. Hutchinson, and A. Cho, Science **264**, 553 (1994).
[35]R. Yang, C. Hill, and B. Yang, Appl. Phys. Lett. **87**, 151109 (2005).
[36]J. Roepcke, G. Lombardi, A. Rousseau, and P. B. Davies, Plasma Sources Sci. Technol. **15**, S148 (2006).
[37]S. Welzel, G. Lombardi, P. B. Davies, R. Engeln, D. C. Schram, and J. Roepcke, J. Appl. Phys **104**, 093115 (2008).
[38]H. Ketelsen, "Mie-Ellipsometrie an Staubigen Plasmen," MSc thesis (University of Kiel, Germany, 2009).
[39]Y. Kabbadj, M. Herman, G. Di Lombardi, L. Fusina, and J. W. Johns, J. Mol. Spectrosc. **150**, 535 (1991).
[40]L. S. Rothman, I. E. Gordon, A. Barbe, D. Chris Benner, P. F. Bernath, M. Birk, V. Boudon, L. R. Brown, A. Campargue, J.-P. Champion, K. Chance, L. H. Coudert, V. Dana, V. M. Devi, S. Fally, J.-M. Flaud, R. R. Gamache, A. Goldman, D. Jacquemart, I. Kleiner, N. Lacome, W. J. Lafferty, J.-Y. Mandin, S. T. Massie, S. N. Mikhailenko, C. E. Miller, N. Moazzen-Ahmadi, O. V. Naumenko, A. V. Nikitin, J. Orphal, V. I. Perevalov, A. Perrin, A. Predoi-Cross, C. P. Rinsland, M. Rotger, M. Šimečková, M. A. H. Smith, K. Sung, S. A. Tashkun, J. Tennyson, R. A. Toth, A. C. Vandaele, and J. Vander Auwera, J. Quant. Spectrosc. Radiat. Transf. **110**, 533 (2009).
[41]J. Berndt, S. Hong, E. Kovacevic, I. Stefanovic, and J. Winter, vacuum **71**, 377 (2003).
[42]S. Dap, D. Lacroix, F. Patisson, R. Hugon, L. de Poucques and J. Bougdira, New J. Phys. **12**, 093014 (2010).
[43]M. Tatanova, Yu B. Golubovskii, A. S. Smirnov, G. Seimer, R. Basner and H. Kersten, Plasma Sources Sci. Technol. **18**, 025026 (2009).
[44]G. Franz and M. Klick, J. Vac. Sci. Technol. A **23**, 917 (2005).
[45]L. Couëdel, M. Mikikian, A. A. Samarian, and L. Boufendi, Phys. Plasmas **17**, 083705 (2010).
[46]S. V. Vladimirov and K. Ostrikov, Phys. Rep. **393**, 175 (2004).
[47]K. N. Ostrikov, S. Kumar, and H. Sugai, Phys. Plasmas **8**, 3490 (2001).
[48]Y. Watanabe, J. Phys. D. Appl. Phys. **39**, R329 (2006).
[49]C. Cui and J. Goree, IEEE Trans. Plasma Sci., **22**, 151 (1994).
[50]Yu. A. Mankelevich, M. A. Olevanov, and T. V. Rakhimova, Plasma Sources Sci. Technol. **17**, 015013 (2008).
[51]Yu. Mankelevich, M. Olevanov, A. Pal', T. Rakhimova, A. Ryabinkin, A. Serov, and A. Filippov, Plasma Phys. Rep. **35**, 191 (2009).
[52]E. Kovacevic, I. Stefanovic, J. Berndt, and J. Winter, J. Appl. Phys. **93**, 2924 (2003).
[53]I. Denysenko, J. Berndt, E. Kovacevic, I. Stefanovic, V. Selenin, and J. Winter, Phys. Plasmas **13**, 073507 (2006); K. N. Ostrikov and M. Y. Yu, J. Phys. D: Appl. Phys. **32**, 1650 (1999).
[54]I. Levchenko, M. Romanov, and M. Keidar, J. Appl. Phys. **94**, 1408 (2003).
[55]K. Ostrikov, H. J. Yoon, A. Rider, and S. V. Vladimirov, Plasma Processes Polym. **4**, 27 (2007).
[56]K. De Bleecker, A. Bogaerts, and W. Goedheer, Phys. Rev. E **73**, 026405 (2006).